Figure 4(b) shows the measured eye diagram of the transmitted bits through the system in Figure 2. The diagram was obtained after superposition of the time period of 100 bits in a single waveform.

The signal-to-noise ratio (SNR) of 40 dB observed in Figure 4(a) can be used to estimate the system maximum achievable BER after considerations of the required baseband filter bandwidth or Nyquist limit (2 MHz), the noise figure of the demodulator circuit (11 dB), and after the assumption is made that the system noise follows a Gaussian distribution. Under these conditions, a propagated SNR of 40 dB for 2-ASK modulation should theoretically be able to achieve BER values below 10^{-9}. These considerations, however, do not take into account the negative impact on BER of undesired effects such as multipath propagation and interchannel interference, which are more difficult to estimate without specific practical considerations.

5. CONCLUSION

Wireless interrogation of an optically modulated RTD-based oscillator has been reported in this article. No errors were found after transmission of 10^6 bits at a data rate of 1 Msym/s. The measurement took place after phase locking of the modulated RTD oscillator and demodulation of the received wireless signal using a commercial circuit. The system RTD technology should be fully scalable to millimetre wave frequency operation where multigigabit data rates can be achieved.

ACKNOWLEDGMENTS

This work was supported by Fundação para a Ciência e a Tecnologia under Project PTDC/EEATEL/100755/2008—WOWi—Wireless–optical–wireless interfaces for picocellular access networks.

REFERENCES

1. P. Agrawal, Fiber-optic communication systems, 3rd ed., Wiley, Hoboken, NJ, 2002.
2. M. Feiginov, C. Sydlo, O. Cojocari, and P. Meissner, Resonant-tunnelling-diode oscillators operating at frequencies above 1.1 THz, Appl Phys Lett 99 (2011), 1–3.
3. H.I. Cantu, B. Romeira, A.E. Kelly, C.N. Ironside, J.M.L. Figueiredo, Resonant tunneling diode optoelectronic circuits applications in radio-over-fiber networks, IEEE Trans Microwave Theory Tech 60 (2012), 2903–2912.

DESIGN AND OPTIMIZATION OF A BROADBAND X-BAND BIDIRECTIONAL AMPLIFIER

Massimo Donelli,[1] Carlos Saavedra,[2] and Md Rukanuzzaman[1]

[1] Department of Information Engineering and Computer Science, University of Trento, Trento, 38100, Italy; Corresponding author: massimo.donelli@dit.unitn.it

[2] Department of Electrical and Computer Engineering, Queen's University, ON, Canada

Received 27 December 2012

ABSTRACT: *This article presents the design of a simple and inexpensive X-band bidirectional amplifier based on two microstrip quadrature hybrid rings and two low cost microwave monolithic integrated circuit monolithic amplifiers. Each subsystem of the amplifier was designed and optimized, by means of an optimization methodology to obtain the best performances. In particular, the design problem was recast as an optimization one by defining suitable cost functions that are then minimized with an evolutionary optimization technique, namely the particle swarm optimizer. An experimental prototype has been designed, developed, and measured. The obtained results demonstrate the capabilities of the proposed broadband bidirectional amplifier and envisage future and possible advances in the application of such devices for the development of advanced telecommunications systems.* © 2013 Wiley Periodicals, Inc. Microwave Opt Technol Lett 55:1730–1735, 2013; View this article online at wileyonlinelibrary.com. DOI 10.1002/mop.27712

Key words: *bidirectional amplifier; optimization techniques; evolutionary algorithms*

1. INTRODUCTION

The design of new microwave circuits and systems is needed in several important areas for civil and military telecommunication systems, industrial and medical equipments. Standard microwave synthesis techniques are quite effective for the design of basic microwave filters [1,2], combiners [3], and broadband couplers [4,5]. Miniaturization, cost reduction, and quick time to market are the challenging issues of nowadays and future research trends in a variety of practical applications ranging from UWB systems [6] to large arrays working at medium and high frequencies, both in civil and military applications. In particular, the design of complex microwave devices such as bidirectional amplifiers [7] is a key issue. Usually, these devices require complex design techniques, high level of expertise and a final tuning phase that dramatically increase the costs and the time to market of the device. In this situation, microwave computer-aided design (CAD) tools [8–10] offer a possible solution to reduce the time to market. In fact, these tools can analyze, design, and modify microwave devices in an unsupervised manner and they necessarily do not request an experienced microwave engineer to operate. In this work, we propose the design of a new inexpensive broadband bidirectional amplifier based on standard microstrip components. In particular, two quadrature hybrid rings, filters, and matching transformers were considered and optimized with an unsupervised methodology based on a powerful evolutionary technique, namely the particle swarm optimizer (PSO) [11–14]. This optimizer has the advantage of escaping local minima, and it is jointly used with a circuital and electromagnetic simulator to maximize the performances of the amplifier.

2. SCHEMATIC OF THE BIDIRECTIONAL AMPLIFIER

The proposed bidirectional amplifier is shown in Figure 1. It includes two microstrip hybrid rings, two amplifiers, a couple of filters, and matching transformers. As it can be noticed from the schematic of Figure 1, in the forward direction the incident signal at port 1 is splitted by the first hybrid ring. Half of the signal power travels on the upper side of the circuit and it is amplified by the forward amplifier. Then the signal reaches the second hybrid ring and half of power reaches port 2, the other half is dissolved by the matching load R_2. While the other half power splitted by the first hybrid is reflected down by the output of the second amplifier and further splitted by the first hybrid, only a quarter of the incident power is reflected down at port 1. The behavior in the reverse direction with the signal that impinges on port 2 is similar. The two passband filters are mandatory to avoid instability when the signal is present in both directions at the same time. As far as the general structure of the considered system is concerned, eight different subsystems have been used. However, considering the symmetry of the structure, the simplicity of the matching transformer and the fact that the off-the-shelf commercial

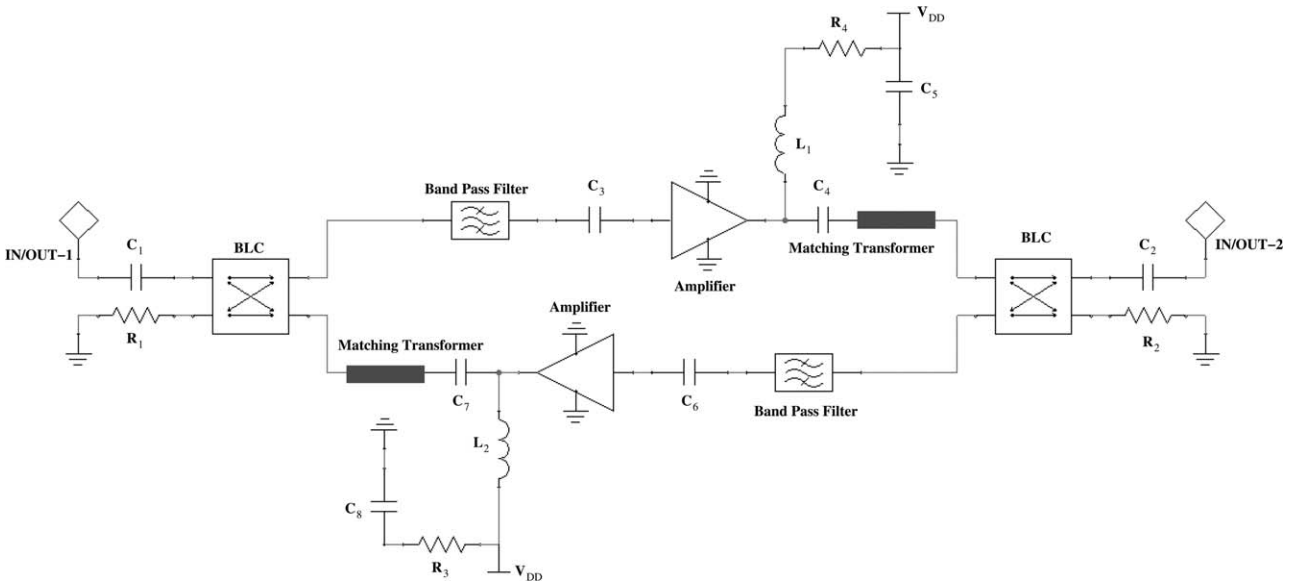

Figure 1 Bidirectional amplifier scheme

amplifier parameters are fixed, only two subsystems have to be accurately characterized (i.e., the filter and the hybrid ring). Moreover, to keep the cost and the simplicity of the system as low as possible, all subsystems will be designed in microstrip technology.

3. THE DESIGN METHODOLOGY

In this section, the considered design methodology for the M subsystems is briefly described. In particular, as reported in the previous section only two microstrip devices are necessary to complete the amplifier: a branch-line coupler and a passband filter. The system must satisfy the following requirements; a gain $G = 10$ dB in both directions, a return loss $S_{11} = S_{22} < -10$ dB, and an insertion loss less than -3 dB. The amplifier must be operative in the X-band in particular a frequency range from 9.0–11.0 GHz is required. Considering that the hybrid must keep a stable behavior for a specific frequency range, a multi arms branch-line coupler is mandatory, in particular a two arms hybrid ring will be considered. Concerning the filter characteristics, a passband filter (mandatory to avoid instabilities when the signal are contemporary introduced into the two input/output ports) with low and high cut-off frequencies at 7.5 and 10.5 GHz is needed. To obtain a compact size device, a stepped impedance resonator passband filter is considered [15]. To design the different subsystems and satisfy the project requirements, the problem at hand is recast as an optimization problem. As the generic system could be composed by subsystems consisting of microstrip structures printed on a planar dielectric substrate or lumped elements circuit, a set of M unknowns vectors are defined $\Gamma = \gamma_1,\ldots,\gamma_{m+1},\ldots\gamma_M$. Each unknown vector γ_m represents the set of geometrical or circuital parameters that define the mth subsystem. During the design phase, M different optimization processes are performed in order to completely design all the subsystems. The optimization processes for the design of the subsystems start from the subsystem requirement vectors $\boldsymbol{\Psi}_m = \left\{ S^m_{p,q}(h\Delta f); m=1,\ldots,N; \quad p,q=1,\ldots,N_m; h=1,\ldots,H \right\} \subset \boldsymbol{\Psi}_{\text{opt}}$, where N and M are the port and subsystems index, respectively. The $\boldsymbol{\Psi}_m$ vectors set the constraint on the scattering parameters, then the following cost function that defines the difference between the subsystem requirements and the trial subsystem solution is considered:

$$\phi\left(\gamma^w_{m,k}\right) = \left\{ \sum_{h=1}^{H} \alpha \left[\sum_{p=1}^{N_m} \max \left[0, \frac{s^{\text{trial}}_{pp}\left(\gamma^w_{m,k}\right) - s^m_{pp}(h\cdot\Delta f)}{s^m_{pp}(h\cdot\Delta f)} \right] \right|_{p=q} + \beta \left[\sum_{i=1}^{N}\sum_{j=1}^{N} \max \left[0, \frac{s^m_{pq}(h\cdot\Delta f) - s^{\text{trial}}_{pq}\left(\gamma^w_{m,k}\right)}{s^m_{pq}(h\cdot\Delta f)} \right] \right|_{p\neq q} \right\} \tag{1}$$

where α and β are two real constants used to weight the different terms of the cost function in Eq. (1). In particular, the α constant is used to weigh the return loss requirement at the ports of the subsystems, while β has been introduced to control the pass-through characteristics of the subsystems. To minimize Eq. (1) and according to the guidelines given in [12], a suitable implementation of the PSO [16] has been used in conjunction with a layout generator and a microwave circuital simulator able to take into account all the characteristics of the subsystems. Starting from each of the trial arrays $\gamma^w_{m,k}$ defined by the PSO, the geometries subsystem generator changes the geometrical or circuital parameters of each subsystem, and then it generates the corresponding subsystem design that satisfies the subsystem requirements. The corresponding scattering parameters, $s^{\text{trial}}_{pp}\left(\gamma^w_{m,k}\right)$, of the subsystem are computed by means of an electromagnetic or a circuital simulator and used to estimate Eq. (1). The iterative process continues until $k = K_{\max}$ or when a convergence threshold on the cost function (1) is reached. Then the array, $\gamma^w_{m,k}$, that contains the geometrical characteristics of the subsystem is stored. When all the M optimizations are complete, all the subsystems are designed and the design procedure

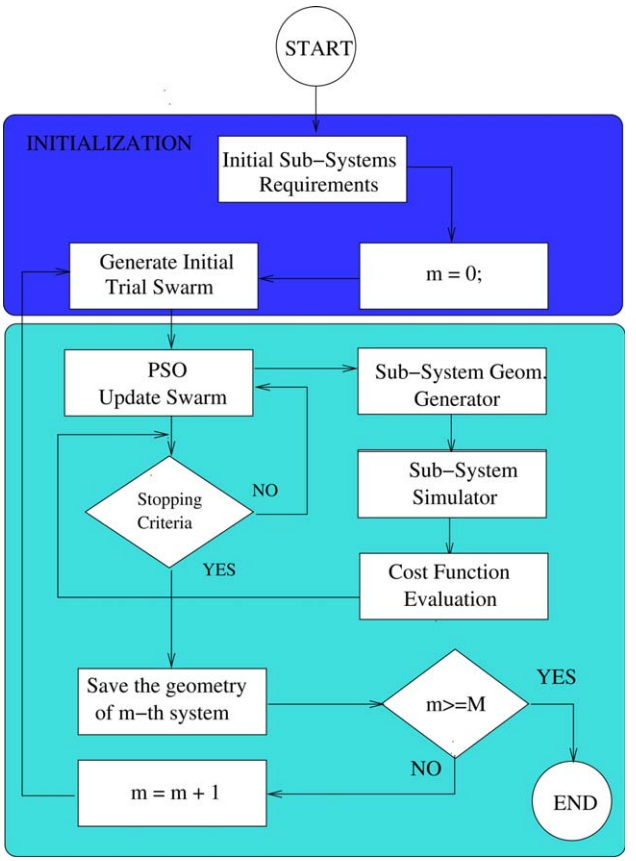

Figure 2 Scheme of the design/optimization loop. [Color figure can be viewed in the online issue, which is available at wileyonlinelibrary.com]

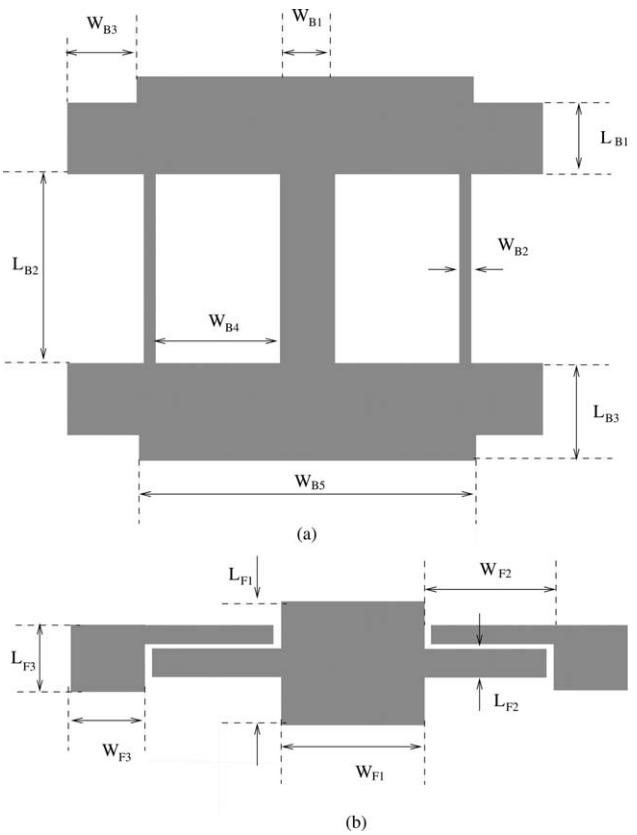

Figure 3 Structure and geometrical parameters of the (a) branch line and (b) passband filter

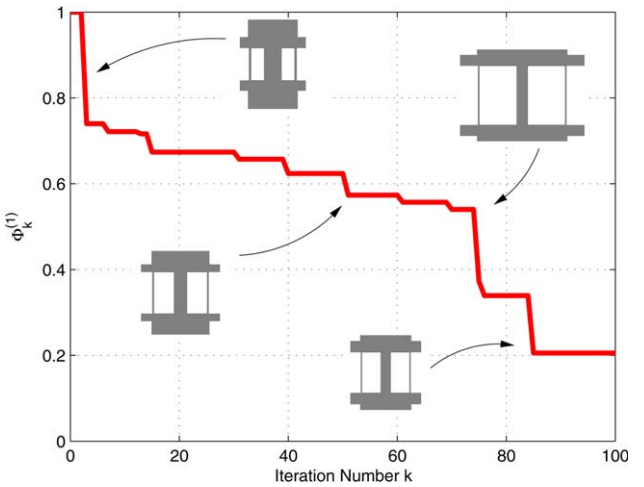

Figure 4 Branch-line design. Behavior of the cost function versus iteration number. Evolution of the hybrid branch-line geometry at different iterations. [Color figure can be viewed in the online issue, which is available at wileyonlinelibrary.com]

ends. It is worth noticing that M optimizations could be performed in a parallel way, in particular following the guidelines reported in [8,17] a strong reduction of the computational time could be obtained. In the following sections, the proposed methodology will be used to design a bidirectional amplifier. The scheme of the considered optimization loop is reported in Figure 2.

3.1. Subsystems Design

In this subsection, the two microstrip devices, namely the multi arms quadrature hybrid and the passband filter, necessary to complete the amplifier scheme will be designed and optimized considering the optimization loop described before. The geometries of the branch line and of the filter are reported in Figures 3(a) and 3(b). Concerning the geometrical parameters, the vector $\mathbf{\Gamma}=\{\gamma_1,\gamma_2,S,l_t,w_t\}$ completely describes the bidirectional amplifier geometry. With reference to Figures 3(a) and 3(b), $\gamma_1=\{W_{b1},L_{b1},W_{b2},L_{b2},W_{b3},L_{b3},W_{b4}\}$ and $\gamma_2=\{W_{f1},L_{f1},W_{f2},L_{f2},W_{f3}\}$ define the branch line and filter geometrical characteristics, respectively. For each of the $M=2$ optimizations required to complete subsystems design, a population composed by $w=5$ trial solutions has been considered. Concerning the other PSO parameters, they have been used the same configuration adopted at the first step. Starting from the requirements for each considered devices expressed by the vector $\mathbf{\Psi_1}=\left\{S^m_{pq}(h\cdot\Delta f);p,q=1,...,N_l=4,;h=1,...,H=100,\right\}$ at $m=1$ provided by the user, the geometry generators produce

TABLE 1 Branchline, Geometrical Parameters Obtained at the End of the Optimization Procedure

W_{b1}	L_{b1}	W_{b2}	L_{b2}	W_{b3}	L_{b4}	W_{b4}	W_{b5}
2.2	2.3	4.5	0.3	2.5	1.8	3.6	10.0

All dimensions are in mm.

TABLE 2 Band Pass Filter, Geometrical Parameters Obtained at the End of the Optimization Procedure

W_{f1}	L_{f1}	W_{f2}	L_{f3}	W_{f3}	L_{f4}	Gap
4.6	5.0	4.5	0.7	4.5	2.5	0.2

All dimensions are in mm.

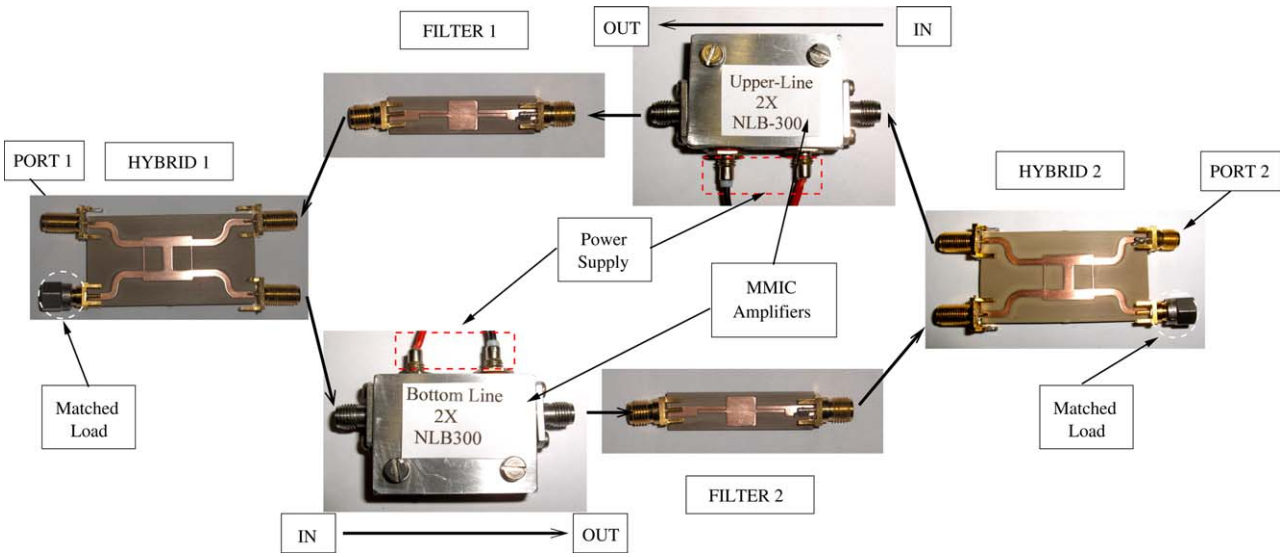

Figure 5 Photography of the completed amplifier prototype. [Color figure can be viewed in the online issue, which is available at wileyonlinelibrary.com]

a set of trial branch-line geometries, that are estimated by means of a (MoM) simulator, which take into account the presence of the dielectric substrate. Then the cost function in Eq. (1) is evaluated and, thanks to the PSO strategy, the swarm evolves improving their characteristics. The iterative procedure continues until the maximum number of iterations or the threshold on the cost function is reached. As an illustrative example of the optimization process, Figure 4 shows the behavior of the cost function versus the iteration number during the optimization of the branch-line geometry; in particular, Figure 4 also reports the geometries of the branch line obtained at different iterations of the optimization procedure. After the design of the hybrid ring, the second step continues with the design of the second subsystem the passband filter. For the filter synthesis, the vector $\mathbf{\Psi}_2 = \left\{ S^2_{pq}(h \cdot \Delta f); p, q = 1, ..., N_1 = 2, ; h = 1, ..., H = 100, \right\}$ at $m = 2$ has been considered and, following the similar optimization procedure adopted for the branch line, a geometry generator generates a trial stepped impedance resonator filter following the geometrical guidelines reported in Figure 3(b), then the MoM engine estimates scattering parameters of the trial solution and the PSO optimizer tries to improve the characteristics of the filter, the procedure is stopped when the best solution satisfies the requirements or the reaching of the maximum number of iterations. As the PSO is a stochastic algorithm, it has been run for 100 times, and a statistical analysis has been performed to demonstrate that the obtained solution is not due to a lucky initialization; in particular, the obtained standard deviation σ is less than 1%. Moreover, for the sake of comparison, the results obtained with the PSO has been compared with those obtained with a gradient-based algorithm (a standard Gauss–Newton algorithm [18]), and other evolutionary algorithms, namely the genetic algorithms [19] and the differential evolution [20]. In all cases, the results obtained with the PSO outperform the other optimization techniques. The geometrical parameters related to the branch line and the band pass filters are summarized in Tables 1 and 2, respectively.

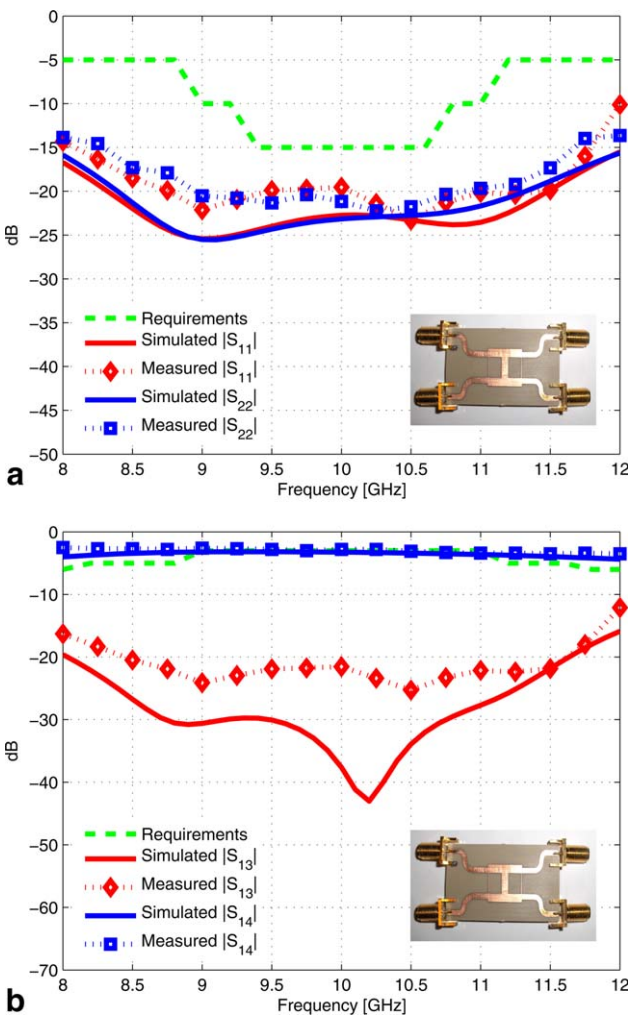

Figure 6 Performances of the optimized branch line. Comparisons with a hybrid ring obtained with a standard design methodology (a) return-loss and isolation and (b) pass-through parameters. [Color figure can be viewed in the online issue, which is available at wileyonlinelibrary.com]

4. EXPERIMENTAL RESULTS

All the subsystems obtained at the end of the design methodology summarized in the previous section have been fabricated

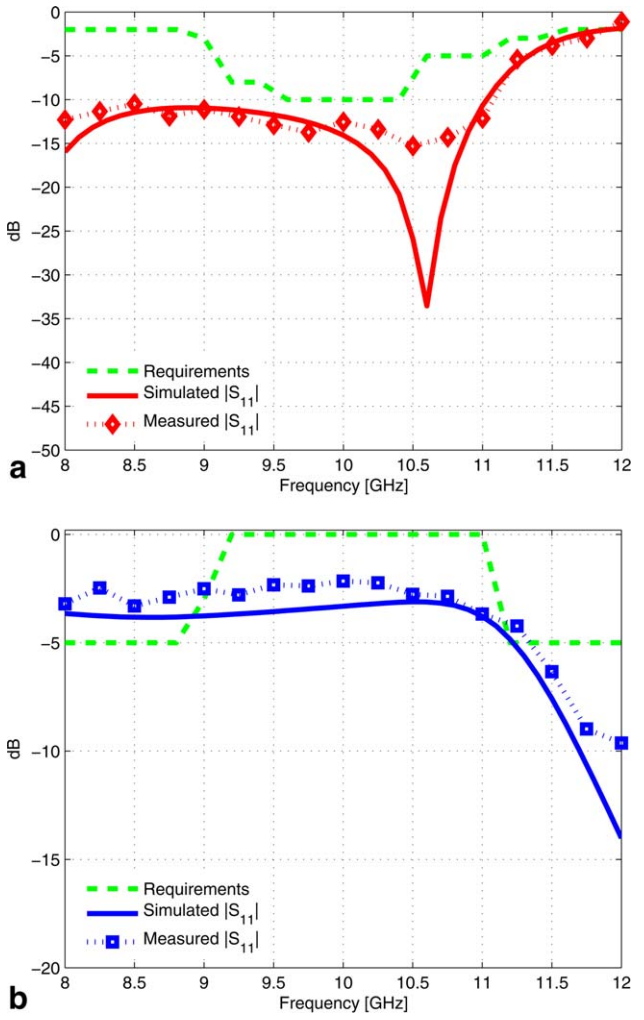

Figure 7 Passband filter design. Return loss and pass-through parameters obtained at the end of the synthesis procedure. (a) Return loss and (b) pass-through parameters. [Color figure can be viewed in the online issue, which is available at wileyonlinelibrary.com]

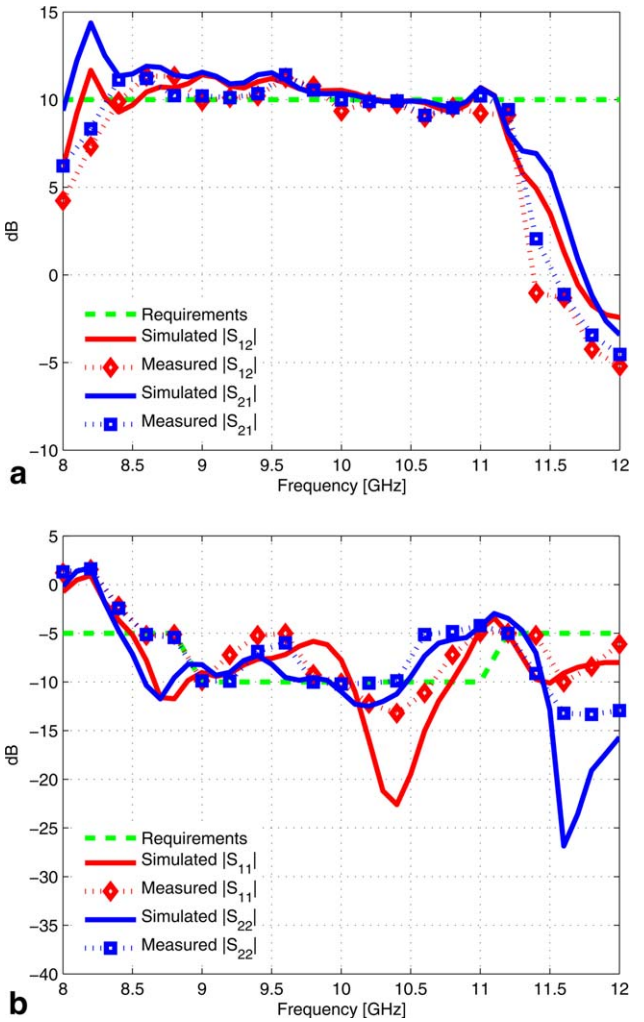

Figure 8 Bidirectional amplifier characteristics. (a) Return loss and (b) pass-through parameters. [Color figure can be viewed in the online issue, which is available at wileyonlinelibrary.com]

with microstrip technology considering a ceramic dielectric material (Arlon 25) able to work in the whole X-band. The microwave monolithic integrated circuit amplifiers have been assembled inside a shielded aluminum box equipped with subminiature type A (SMA) connectors. In particular, two NLB-300 amplifiers, from Minicircuits, connected in cascade have been used to obtain the required gain. The shielded boxes used for the upper/lower line of the bidirectional amplifier contain the bias networks and the decoupling capacitors and inductors necessary to properly provide the power supply to the amplifiers. Figure 5 shows the photo of each subsystem including the two shielded boxes that contain the amplifiers. Each subsystem was individually tested for performance verification purposes using a network analyzer and the measurements were compared with the simulated data. Then, the bidirectional amplifier was assembled connecting all the subsystems with rigid cables following the schematic reported in Figure 1. Figures 6 and 7 report the comparisons between the simulated and measured data concerning the return loss, the isolation and the pass-through parameters of the hybrid ring, respectively. As can be noticed from the data reported in Figure 8, the obtained hybrid branch-line geometry satisfies the project requirements. In particular, pass-through parameters reached the -3 dB values, and they keep a flat behavior in the whole frequency range of interest [Figure 6(b)]. Moreover, the return loss and the isolation parameters are below the required thresholds in the whole frequency range of interest [Figure 6(a)]. The characteristics of the passband filter prototype are reported and compared with the numerical simulation in Figure 6. The obtained experimental results are satisfactory; in particular, the return loss reported in Figure 7(a) perfectly agree with the requirements, also the agreement between measured and simulated data of pass-through parameter reported in Figure 7(b) is satisfactory, a slight attenuation of about 2 dB can be observed between 8 and 11 GHz. The last step of the assessment is to connect together all the subsystems to obtain the bidirectional amplifier; to do this, rigid cables equipped with SMA connectors have been used. Once assembled, the bidirectional amplifier has been measured with a network analyzer and the obtained measures compared with numerical data obtained with a commercial simulator (Ansoft Nexim). The data are reported in Figure 8, in particular Figure 8(a) shows the gain of the amplifier in both directions. As it can be noticed from the data reported in Figure 8(a), the gain of the amplifier is slightly above $+10$ dB from 8.5 GHz up to about 11 GHz. However, the gain of the amplifier is quite flat. The return loss measured at the two ports of the amplifier is reported in Figure 8(b); as it can be noticed, the results are

satisfactory, in particular between 10 and 11 GHz the return loss is slightly below −10dB, while between 9 and 10 GHz the return loss performances get worse reaching about −5 dB. The return loss could be improved by inserting suitable devices able to reduce the reflected signal at the output of the two amplifiers, in particular two circulators could improve the return loss of the bidirectional amplifier, but the introduction of such kind of a device can improve too much the cost of the device. However, the performances of the obtained amplifier can be considered satisfactory considering the simplicity and the cheapness of the obtained prototype, and they demonstrate the potentialities of the proposed CAD tools for the design of complex microwave devices.

5. CONCLUSION

In this work, a bidirectional amplifier able to amplify the signals in both directions at the same time and able to operate in a wide frequency band has been designed, fabricated, and experimentally assessed. The design methodology was based on an unsupervised technique. In particular, starting from the design requirements each subsystem has been designed and optimized by means of a powerful optimization algorithm namely the PSO. The measured results of the amplifier prototype demonstrated the capabilities and the efficacy of the proposed scheme and of the design methodology. Future work will be aimed at the improvement of the tool performances, in particular to reduce the computational time required by the synthesis method, parallel computation will be considered.

REFERENCES

1. D. Pozar, Microwave engineering, Wiley, New York, 1998.
2. Y. Kuo and C.Y. Chang, Analytical design of two-mode dual band filters using e-shaped resonators, IEEE Trans Microwave Theory Tech 9 (2001), 476–479.
3. S. Kumar, C. Tannous, and T. Danshin, A multisection broadband impedance transforming branch-line hybrid, IEEE Trans Microwave Theory Tech 43 (1995), 2517–2523.
4. K. Wincza and S. Gruszczynski, Miniaturized quasi-lumped coupled-line single section and multisection directional couplers, IEEE Trans Microwave Theory Tech 48 (2010), 2924–2931.
5. Y.C. Chiang and C.Y. Chen, Design of a wideband lumped-element 3-dB quadrature coupler, IEEE Trans Microwave Theory Tech, 9 (2001), 476–479.
6. X. Huang, C. Cheng, and L. Zhu, An ultrawideband (UBW) slotline antenna under multiple-mode resonance, IEEE Trans Antennas Propag 60 (2012), 385–389.
7. S. Chung, S. Chen, and Y. Lee, A novel bi-directional amplifier with applications in active Van Atta retrodirective arrays, IEEE Trans Microwave Theory Tech 51 (2003), 542–547.
8. S. Caorsi, M. Donelli, A. Massa, and M. Raffetto, A parallel implementation of an evolutionary-based automatic tool for microwave circuit synthesis: Preliminary results, Microwave Opt Technol Lett 35 (2002).
9. M. Donelli, R. Azaro, A. Massa, and M. Raffetto, Unsupervised synthesis of microwave components by means of an evolutionary-based tool exploiting distributed computing resources. Prog Electromagn Res 56 (2006), 93–108.
10. R. Azaro, F. De Natale, M. Donelli, and A. Massa, PSO-based optimization of matching loads for lossy transmission lines, Microwave Opt Technol Lett 48 (2006), 1485–1487.
11. J. Kennedy, R.C. Eberhart, and Y. Shi, Swarm intelligence, San Francisco, Morgan Kaufmann, 2001.
12. J. Robinson and Y. Rahmat-Samii, Particle swarm optimization in electromagnetics, IEEE Trans Antennas Propag 52 (2004), 397–407.
13. M. Donelli and A. Massa, A computational approach based on a particle swarm optimizer for microwave imaging of two-dimensional dielectric scatterers, IEEE Trans Microwave Theory Tech 53 (2005), 1761–1776.
14. M. Clerc and J. Kennedy, The particle swarm—Explosion, stability, and convergence in a multidimensional complex space, IEEE Trans Evol Comput 6, 58–73.
15. C. Hung, M. Weng, Y. Su, and R. Yang, Design of design of parallel coupled-line microstrip wideband bandpass filter using stepped-impedance resonators, Microwave Opt Technol Lett 49 (2007), 795–798.
16. R. Azaro, F. De Natale, M. Donelli, and E. Zeni, Optimized design of a multi-function/multi-band antenna for automotive rescue systems, IEEE Trans Antennas Propag 54 (2006), 897–904.
17. A. Massa, D. Franceschini, G. Franceschini, M. Pastorino, M. Raffetto, and M. Donelli, Parallel GA-based approach for microwave imaging applications, IEEE Trans Antennas Propag 53 (2005), 3118–3127.
18. B.N. Pshenichny and Y.M. Danilin, Numerical method in extremal problems, Mir Edition, Moscow, 1978.
19. J.H. Holland, Genetic algorithm, Addison Wesley, Reading, MA, 1989.
20. K. Price, R. Storn, and J. Lampinen, Differential evolution—A practical approach to global optimization, Springer, New York, NY, 2005.

FLEXIBLE FABRICATION OF LONG-PERIOD FIBER GRATING DEVICES BASED ON ERASING EFFECT BY CONTROLLED CO_2 LASER PULSE EXPOSURE

Baokai Cheng, Xinwei Lan, Jie Huang, Xia Fang, and Hai Xiao
Department of Electrical Engineering, Missouri University of Science and Technology, Rolla, MO; Corresponding author: xiaoha@mst.edu

Received 28 December 2012

ABSTRACT: *An easy way to flexibly fabricate special long-period fiber grating (LPFG) devices by controlled CO_2 laser pulses are presented in this paper. By controlling the pulse power and duration, consecutive exposures were made on an optical fiber to fabricate an LPFG. Existing LPFGs can also be erased or modified by applying CO_2 laser exposures on specific grating sections. The erasing effect has been studied to fabricate special grating devices for various applications.* © 2013 Wiley Periodicals, Inc. Microwave Opt Technol Lett 55:1735–1738, 2013; View this article online at wileyonlinelibrary.com. DOI 10.1002/mop.27711

Key words: *CO_2 laser fabrication; erasing effect; fiber grating; fiber interferometer; phase shifted grating*

1. INTRODUCTION

Long-period fiber gratings (LPFGs) are in-fiber devices that have periodic perturbation of refractive index along the optical fiber [1, 2]. They have a periodicity of about several hundred microns which give them the characteristic of coupling propagating core mode to cladding modes. Besides their wide applications as components in communication systems, they are also popular in sensor systems as they can respond to the environment conditions, such as temperature and stress change [3, 4].

Because of the low cost of optical fiber and the wide applications of LPFGs, a lot of studies have been done on their fabrication methods. Currently, several methods have been used to write LPFGs, including the usage of laser exposure, mechanical deformation and electric arc, and so forth. Among them, laser exposure is most popular because it has low loss and introduces almost no mechanical defects to fiber. The laser sources include UV lasers, CO_2 lasers, and femtosecond lasers, and the fabrication method can be classified into amplitude mask method and point-by-point fabrication method [1, 5–8]. Among the laser sources, CO_2 laser has lower cost and is easy to setup. As for fabrication method, because amplitude masks are premade, it is not easy to tune grating period with them, hence the point-by-point fabrication methods are more common [9, 10]. However, one of the problems of these methods is that they lack fabrication flexibility.